Changes in the global carbon cycle occurred as two episodes during the Permian–Triassic crisis

Article *in* Geology · December 2007

DOI: 10.1130/G24224A.1

9 authors, including:

Shucheng Xie
China University of Geosciences

Paul B Wignall
University of Leeds

Xianyu Huang
China University of Geosciences

Xulong Lai
China University of Geosciences

Changes in the global carbon cycle occurred as two episodes during the Permian–Triassic crisis

Shucheng Xie — Key Laboratory of Biogeology and Environmental Geology of Ministry of Education, and State Key Laboratory of Geological Processes and Mineral Resources, China University of Geosciences, Wuhan 430074, People's Republic of China
Richard D. Pancost — Bristol Biogeochemistry Center, School of Chemistry, University of Bristol, Cantock's Close BS8 1TS, Bristol, UK
Junhua Huang — State Key Laboratory of Geological Processes and Mineral Resources, China University of Geosciences, Wuhan 430074, People's Republic of China
Paul B. Wignall — School of Earth and Environment, University of Leeds, LS2 9JT, Leeds, UK
Jianxin Yu, Xinyan Tang, Lin Chen, Xianyu Huang, Xulong Lai — Key Laboratory of Biogeology and Environmental Geology of Ministry of Education, China University of Geosciences, Wuhan 430074, People's Republic of China

ABSTRACT

Coeval records of ocean, atmosphere, and terrestrial change are crucial to understanding the pattern and causes of global mass extinction across the Permian-Triassic boundary (PTB). However, relationships among changes in different settings remain largely unclear, primarily due to the challenges associated with the correlation among disparate records. Here we compare marine carbon isotopic records with marine and terrestrial environmental and biotic events recorded in sediments from the Meishan PTB section of south China. Time-scaled carbonate carbon isotopes exhibit two gradual major shifts across the PTB at Meishan, and these are duplicable elsewhere around the Tethys Ocean. The two shifts are associated with two episodes of enhanced terrestrial weathering indicated by an increased abundance of ^{13}C-enriched moretanes relative to hopanes and an elevated abundance of black carbon fragments. Key marine events previously reported for the PTB, including photic zone euxinia, faunal mass extinction, and cyanobacterial expansion, also occur as two episodes, coinciding with both of the progressive shifts to negative δ^{13}C values and enhanced weathering. The temporal sequence of the duplicable events suggests that the biotic crisis was a consequence of prolonged and episodic changes in the marine and continental systems, and argues against an extraterrestrial impact as the main cause.

Keywords: carbon cycle, biomarker, conodont, Permian-Triassic boundary, extinction.

INTRODUCTION

Recently developed biological and geochemical records of the Permian-Triassic boundary (PTB) have provided an enhanced understanding of the pattern and potential causes of the PTB faunal mass extinction. Among the geochemical records, the carbonate carbon isotope record is of particular importance and widely explored because it is recorded in marine and terrestrial settings, allowing a global correlation (Baud et al., 1989; Jin et al., 2000; Payne et al., 2004; Riccardi et al., 2007). Two shifts in carbonate δ^{13}C values have been observed in the Austrian PTB sediment record (Holser et al., 1989), but that record's global significance and its correlation with marine and terrestrial biological events have yet to be explored. We have developed a high-resolution time-scaled carbonate δ^{13}C record in Meishan sediments. The resulting records, along with conodont biostratigraphy, are correlated to different sections from the Tethyan region. The isotope records are further compared to a range of oceanographic, biotic, and continental changes that occurred across the PTB, enabling an enhanced understanding of environmental change at that time.

CARBON ISOTOPE PROFILES

Bulk carbonate δ^{13}C values range from –1.3‰ to 4.8‰ in the interval investigated (Fig. 1) and show no correlation ($R^2 = 0.002$) with δ^{18}O values. An excursion in δ^{13}C values occurs in the highly condensed beds 25–26 below the PTB (Fig. 1), corresponding to the well-known end-Permian shift that has been documented globally. However, one of the most remarkable features in the isotope profile is the occurrence of a second major shift spanning beds 28–37. Thus, the time-scaled profile (Fig. 2), developed on the basis of the absolute radiometric dating of volcanic ash at Meishan (Bowring et al., 1998), clearly reveals two significant shifts in δ^{13}C values: a progressive decline from 4.8‰ (bed 23) to –0.6‰ (bed 26) (episode I, Fig. 2) in the *Clarkina meishanensis* conodont zone (Tong and Yang, 1999), followed by a second progressive shift from 1.4‰ (bed 28) to –1.3‰ (bed 34) in the *Isarcicella isarcica* zone (episode II). It is critical that the occurrence of two (as opposed to a single) negative carbon isotope excursions across the PTB is also apparent in two other Tethyan sections (Fig. 2): the Carnic Alps, Austria, representing the Eurasian Tethys (Holser et al., 1989), and Shahreza, central Iran, representing the Gondwanan Tethys (Korte et al., 2004). The three sections can be correlated using conodont biostratigraphy (Schönlaub, 1991; Tong and Yang, 1999; Korte et al., 2004), further supporting comparison of the three carbon isotopic profiles (although some differences could result from regional variability). Our work, for the first time, duplicates the two shifts in Austria at the global stratotype section and point, allowing precise global correlation among marine PTB sites.

At all three sections, both episodes exhibit gradual rather than abrupt shifts. The gradual shift during episode I has been documented at a wide variety of sections and is believed to be a global characteristic of the latest Permian oceans (Payne et al., 2004; Haas et al., 2007). Previously, a sharp drop in δ^{13}C values within bed 25 followed by an immediate recovery at bed 26 was reported at Meishan (Jin et al., 2000). However, our data reveal that both beds 25 (white volcanic ash) and 26 (black calcareous clay) have similar ranges of δ^{13}C values (Fig. 1). Our lowest δ^{13}C value for bed 25 is ~1‰ greater than that previously reported (Jin et al., 2000); the previously reported low δ^{13}C values were strictly confined to a lithologic boundary between a limestone (bed 24) and a volcanic ash clay (bed 25), where postdepositional weathering could have occurred and biased the signal. Moreover, our new Meishan data are consistent with a recent report from Hungarian sections, where a negative shift has been correlated to bed 26 at Meishan (Haas et al., 2007). Our negative values at bed 26, coinciding with cyanobacterial blooms (Xie et al., 2005), appear to match end-

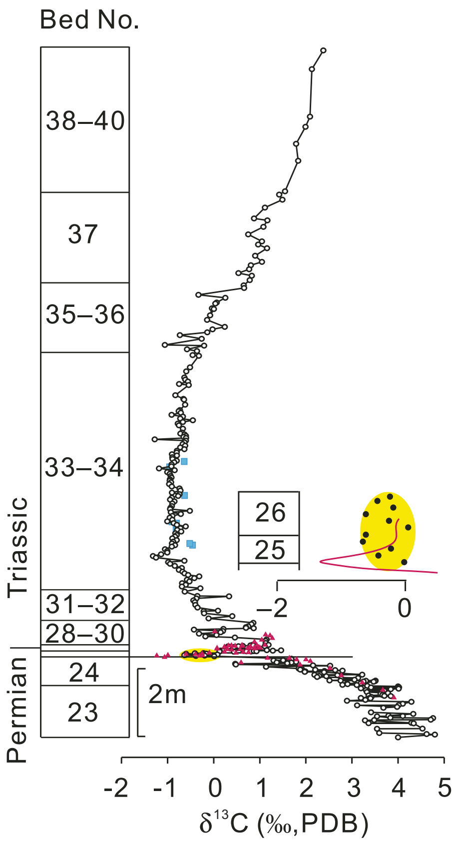

Figure 1. Profile of the high-resolution record of marine carbonate δ¹³C values (PDB—Peedee belemnite) at Meishan, south China. The δ¹³C values of beds 25 and 26 are circled in yellow area and shown in expanded profile. Blue solid blocks are used to show carbonate δ¹³C data in distinct lithologies (muddy limestones and calcareous claystones) of bed 34. Red triangles and red curve show data and trend as reported by Jin et al. (2000).

Permian δ¹³C minima observed within microbialite beds in Nanpanjiang, south China (Payne et al., 2004). Thus, the gradual shift in carbonate δ¹³C values reported here (bed 24 to bed 26) appears to be a robust record of regional and perhaps global environmental change. This continuous δ¹³C drop suggests that environmental perturbation in the latest Permian occurred more gradually than previously suggested (Jin et al., 2000), and there is no compelling need to invoke a catastrophic event, such as a bolide impact or methane hydrate release, for the observed shift.

BIOMARKER RECORDS OF ENHANCED TERRESTRIAL WEATHERING

Significantly, both of the negative carbon isotope excursions coincide with elevated concentrations of the 17β(H),21α(H) isomers of hopanes (moretanes) relative to 17α(H),21β(H) hopanes, with the ratios initially increasing in bed 24 (Fig. 3; shown as C_{29} or C_{30} moretane to C_{30} hopane ratios). Although the relative moretane abundance is affected by thermal maturity, the narrow stratigraphic intervals examined here and the invariant temperature of maximum pyrolysis (Xie et al., 2005) preclude that as an explanation for large differences in Meishan moretane/hopane ratios.

Enhanced moretane abundance during episode I was reported at Meishan (Wang, 2007), comparable to our data (Fig. 3); that study proposed either enhanced terrestrial inputs or marine acidification as two possible mechanisms. However, high acidity favors the rapid formation of 17α(H),21β(H) hopanes (Ries-Kautt and Albrecht, 1989; Dehmer, 1995). Alternatively, the maxima in moretane relative abundances coincide with decreased deposition of carbonate, suggesting that lithology could be a primary control on moretane/hopane ratios; however, despite a surficial similarity, the two geochemical records are not correlated. For example, the maximum of moretane abundance during episode I (0.4) is much lower than that during episode II (1.1), although both sediments have comparably low carbonate contents. Within episode II, carbonate contents are lower in beds 29–34, but the moretane abundance peaked at bed 34.

Alternatively, relatively high moretane to hopane ratios have been observed in terrestrial sediments and marine sediments with high terrestrial inputs (Grantham, 1986; Peters et al., 2005). Moreover, moretane precursors such as 17β(H),21α-moretan-29-ol and 17β(H)-moret-22(29)-ene have been reported from terrestrial environments (Quirk et al., 1984; Uemura and Ishiwatari, 1995). Thus, increased terrestrial inputs have previously been proposed to explain high relative abundances of moretanes (Grantham, 1986). In Meishan PTB sediments, C_{30} moretane is 1‰–2‰ enriched in ^{13}C relative to C_{30} hopane (see GSA Data Repository Appendix[1]); similarly, PTB terrestrial organic matter δ¹³C values are greater than those of contemporaneous marine organic matter (Riccardi et al., 2007). Thus, our compound-specific isotope data provide further evidence that the enhanced abundance of moretanes records increased terrestrial inputs. Consistent with this interpretation, enhanced relative abundances of moretanes were previously observed in association with a global terrestrial catastrophe in PTB sections in Italy (Watson et al., 2005). Furthermore, widespread increases in continental weathering at the PTB have previously been inferred from end-

[1]GSA Data Repository item 2007269, Appendix (lithology and methods), is available online at www.geosociety.org/pubs/ft2007.htm, or on request from editing@geosociety.org or Documents Secretary, GSA, P.O. Box 9140, Boulder, CO 80301, USA.

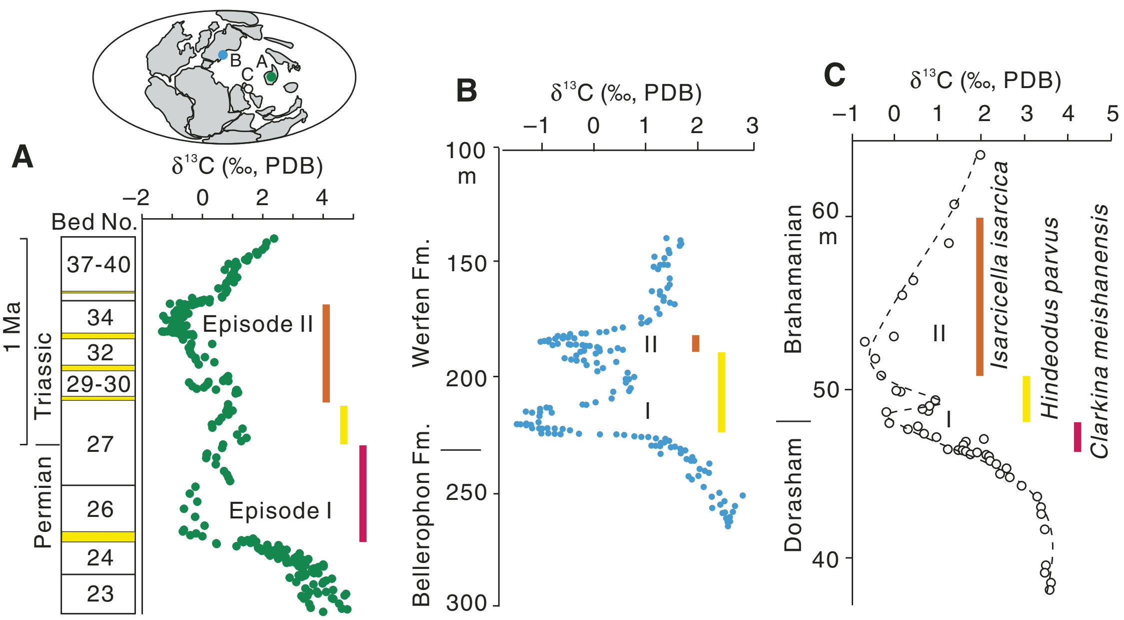

Figure 2. Time-scaled profile of carbonate δ¹³C (PDB—Peedee belemnite) values at Meishan (A) and its biostratigraphy-based correlation with δ¹³C values of the GK-1 core in the Carnic Alps, Austria (B) (Holser et al., 1989), and the Shahreza section in central Iran (C) (Korte et al., 2004). Colored lines show distribution ranges of the three conodont zones for the profiles (Schönlaub, 1991; Tong and Yang, 1999; Korte et al., 2004). Yellow bars associated with the bed numbers denote volcanic ash beds. Paleogeography is after Erwin (1994).

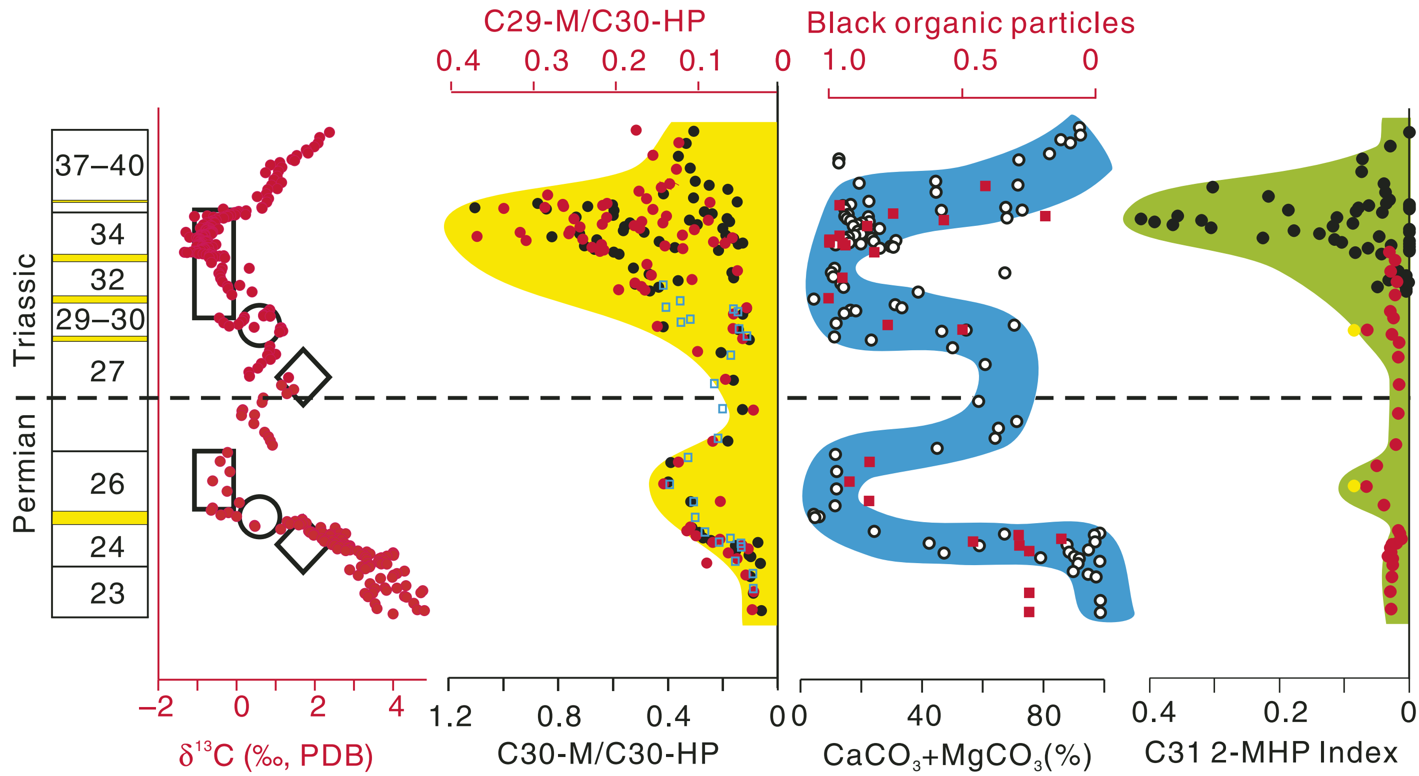

Figure 3. Profiles showing the two changes in multiple biological and environmental parameters in the Meishan section. δ^{13}C represents the carbon isotopic composition of bulk carbonate (PDB—Peedee belemnite). Horizons of the two episodic changes in photic zone euxinia (Grice et al., 2005), faunal turnover (Jin et al., 2000; Xie et al., 2005), and cyanobacterial expansion are denoted by the open diamonds, circles, and blocks, respectively. C30-M/C30-HP or C29-M/C30-HP represents the ratio of C_{30} moretane (C30-M) or C_{29} moretane (C29-M) to C_{30} hopane (C30-HP). Blue open blocks show data from Wang (2007). Black organic particles (red squares) show abundance of wildfire-related black carbonaceous fragments relative to all higher plant materials, expressed by ratio of black carbonaceous fragments to total grains derived from higher plants (Appendix; see footnote 1). Sum of $CaCO_3$ and $MgCO_3$ shows content (%) of carbonate. Cyanobacterial C_{31} 2-methylhopane (2-MHP) index is expressed by C_{31} 2-methylhopane/(C_{31} 2-methylhopane + C_{30} hopane); data in red are from Xie et al. (2005) and data in yellow are from Wang (2007).

Permian pedoliths (Retallack, 1998) and furan-containing compounds (Sephton et al., 2005). The two δ^{13}C minima and the two maxima of moretane abundance could record enhanced continental erosion throughout Pangea.

The two episodes are also associated with elevated concentrations of black organic particles relative to the total amount of higher plant fragments (Fig. 3), indicating the prevalence of wildfires during these two events at Meishan. The relative abundance (expressed as a proportion of the higher plant materials) used here excludes the possibility of the contribution arising from local changes in the balance of marine and terrestrially derived sediments because both the black organic fragments and higher plant materials have a terrigenous origin. The black organic record at Meishan, together with the high charcoal content observed in a west Australian core (Thomas et al., 2004), suggests that PTB weathering could have been enhanced by wildfires.

The two carbon isotope and biomarker ratio shifts coincide with peaks of extinction probability, the first removing many taxa during the main phase of the end-Permian extinction and the latter removing most Permian holdover taxa (Xie et al., 2005). However, the changes in the continent appear to have been more dramatic during episode II. The increases in moretane to hopane ratios are about three times greater during episode II than during episode I. The dramatic change is further indicated by the remarkable increase in 2-methylhopane indices (Fig. 3), possibly resulting from a cyanobacterial response to nutrient inputs from the continent. This suggests that the continental environmental disaster was more severe after the main marine crisis.

TWO CHANGES WITHIN THE LAND-SEA-ATMOSPHERE SYSTEM

Compiling the new isotopic and biomarker records with previously described records from Meishan allows a temporal sequence of environmental and biotic change to be developed (Fig. 3). It is noteworthy that all of these events occur in a specific order that is repeated twice in the Meishan sections; these changes start with a gradual increase in terrestrial weathering (as inferred from moretane abundance), followed by photic zone euxinia at beds 24 and 27 as revealed by green sulfur bacterial biomarkers, (isorenieratane; Grice et al., 2005), faunal mass extinction at beds 25–26 and 28–29 as indicated by extinction probability (Jin et al., 2000; Xie et al., 2005), and cyanobacterial expansion at beds 26 and 29–34 as shown by 2-methylhopane indices (Fig. 3).

A causal relationship between changes in the carbon cycle and Siberian flood basalts has been suggested (Payne and Kump, 2007). The episodic eruptions of Siberian volcanism (Payne and Kump, 2007), such as the main eruption corresponding to the Maymecha-Kotuy volcanic sequence followed by another episode corresponding to the Guli complex (Kamo et al., 2003), could explain the paired continental and marine changes as reconstructed at Meishan sections. The introduction of volcanogenic gases into the atmosphere could have caused a negative shift in the carbon isotopic composition of the ocean-atmosphere reservoir (Payne and Kump, 2007), as recorded in beds 24–26. Beerling et al. (2007) further proposed that the release of organohalogens by the Siberian Traps may have severely weakened the ozone layer, to the detriment of plant life. Large tracts of dead vegetation would have then been subject to extensive wildfires, as recorded in the Meishan record. This, in turn, could have caused terrestrial weathering to increase, starting at bed 24 and peaking at bed 26. The enhanced weathering would have released more ^{13}C-depleted carbon, contributing further to the negative carbon isotope excursion. High pCO_2 would have raised global temperatures (Wignall and Twitchett, 1996), and this could have favored development of global oceanic anoxia (Hotinski et al., 2000), as observed at bed 24 (Grice et al., 2005). The integrated effects induced by volcanism (elevated pCO_2 and associated global warming, marine anoxia/toxic H_2S) (Hotinski et al., 2000; Grice et al., 2005; Knoll et al., 2007), led to, ecologically and physiologically, faunal mass extinction at beds 25–26, with subsequent cyanobacterial expansion at bed 26 arising due to enhanced nutrient inputs and/or the release of grazing pressure (Xie et al., 2005).

Another episode of volcanism (Kamo et al., 2003) could have caused the second almost identical sequence of changes (episode II), albeit one with an apparently more dramatic collapse of the terrestrial ecosystem. These patterns are consistent with neither a massive hydrate release nor a bolide impact as being proximal causes of the extinction. Instead, the most voluminous and explosive continental volcanic event of the Phanerozoic record is a likely cause for the most severe biotic crisis and the changes in the marine and terrestrial realms.

ACKNOWLEDGMENTS

We thank Y. Yi, Y. Pu, and D. Jiao for field assistance in sampling. We are indebted to David Bottjer, Lee Kump, Richard Evershed, Jonathan Payne, Pedro Marenco, Hongfu Yin, and an anonymous reviewer for critical comments that greatly improved an earlier version of the manuscript. This work was supported by the National Natural Science Foundation of China (40525008, 40621002), the Ministry of Education (NCET-04-0729, IRT0546), and the SinoPec project of the China Petroleum and Chemical Corporation (G0800-06-ZS-319).

REFERENCES CITED

Baud, A., Magaritz, M., and Holser, W.T., 1989, Permian-Triassic of the Tethys: Carbon isotope studies: Geologische Rundschau, v. 78, p. 649–677, doi: 10.1007/BF01776196.

Beerling, D.J., Harfoot, M., Lomax, B., and Pyle, J.A., 2007, The stability of the stratospheric ozone layer during the end-Permian eruption of the Siberian Traps: Royal Society of London Philosophical Transactions, ser. A, v. 365, p. 1843–1866.

Bowring, S.A., Erwin, D.H., Jin, Y.G., Martin, M.W., Davidek, K., and Wang, W., 1998, U/Pb zircon geochronology and tempo of the end-Permian mass extinction: Science, v. 280, p. 1039–1045, doi: 10.1126/science.280.5366.1039.

Dehmer, J., 1995, Petrology and organic geochemical investigation of recent peat with known environments of deposition: International Journal of Coal Geology, v. 28, p. 111–138, doi: 10.1016/0166–5162(95)00016-X.

Erwin, D.H., 1994, The Permo-Triassic extinction: Nature, v. 367, p. 231–236, doi: 10.1038/367231a0.

Grantham, P.J., 1986, Sterane isomerisation and moretane/hopane ratios in crude oils derived from Tertiary source rocks: Organic Geochemistry, v. 9, p. 293–304, doi: 10.1016/0146–6380(86)90110–5.

Grice, K., Cao, C., Love, G.D., Böttcher, M.E., Twitchett, R.J., Grosjean, E., Summons, R.E., Turgeon, S.C., Dunning, W., and Jin, Y., 2005, Photic zone euxinia during the Permian-Triassic superanoxic event: Science, v. 307, p. 706–709, doi: 10.1126/science.1104323.

Haas, J., Demény, A., Hips, K., Zajzon, N., Weiszburg, T.G., Sudar, M., and Pálfy, J., 2007, Biotic and environmental changes in the Permian–Triassic boundary interval recorded on a western Tethyan ramp in the Bükk Mountains, Hungary: Global and Planetary Change, v. 55, p. 136–154, doi: 10.1016/j.gloplacha.2006.06.010.

Holser, W.T., Schönlaub, H.-P., Attrep, M., Jr., Boeckelmann, K., Klein, P., Magaritz, M., Orth, C.J., Fenninger, A., Jenny, C., Kralik, M., Mauritsch, H., Pak, E., Schramm, J.-M., Stattegger, K., and Schmöller, R., 1989, A unique geochemical record at the Permian/Triassic boundary: Nature, v. 337, p. 39–44, doi: 10.1038/337039a0.

Hotinski, R., Kump, L., and Najjar, R., 2000, Opening Pandora's Box: The impact of open-system modeling on interpretations of anoxia: Paleoceanography, v. 15, p. 267–279, doi: 10.1029/1999PA000408.

Jin, Y.G., Wang, Y., Wang, W., Shang, Q.H., Cao, C.Q., and Erwin, D.H., 2000, Pattern of marine mass extinction near the Permian-Triassic boundary in South China: Science, v. 289, p. 432–436, doi: 10.1126/science.289.5478.432.

Kamo, S.L., Czamanske, G.K., Amelin, Y., Fedorenko, V.A., Davis, D.W., and Trofimov, V.R., 2003, Rapid eruption of Siberian flood-volcanic rocks and evidence for coincidence with the Permian-Triassic boundary and mass extinction at 251 Ma: Earth and Planetary Science Letters, v. 214, p. 75–91, doi: 10.1016/S0012–821X(03)00347–9.

Knoll, A.H., Bambach, R.K., Payne, J.L., Pruss, S., and Fischer, W.W., 2007, Paleophysiology and end-Permian mass extinction: Earth and Planetary Science Letters, v. 256, p. 295–313, doi: 10.1016/j.epsl.2007.02.018.

Korte, C., Kozur, H.W., and Mohtat-Aghai, P., 2004, Dzhulfian to lowermost Triassic delta 13C record at the Permian/Triassic boundary section at Shahreza, Central Iran: Hallesches Jahrbuch für Geowissenschaften, Reihe B, Beiheft, v. 18, p. 73–78.

Payne, J.L., and Kump, L.R., 2007, Evidence for recurrent Early Triassic massive volcanism from quantitative interpretation of carbon isotopic fluctuations: Earth and Planetary Science Letters, v. 256, p. 264–277, doi: 10.1016/j.epsl.2007.01.034.

Payne, J.L., Lehrmann, D.J., Wei, J., Orchard, M.J., Schrag, D.P., and Knoll, A.H., 2004, Large pertubations of the carbon cycle during recovery from the end-Permian extinction: Science, v. 305, p. 506–509, doi: 10.1126/science.1097023.

Peters, K.E., Walters, C.C., and Moldowan, J.M., 2005, The biomarker guide—Volume II, Biomarkers and isotopes in petroleum exploration and earth history (second edition): Cambridge, Cambridge University Press, 679 p.

Quirk, M.M., Wardroper, A.M.K., Wheatley, R.E., and Maxwell, J.R., 1984, Extended hopanoids in peat environments: Chemical Geology, v. 42, p. 25–43, doi: 10.1016/0009–2541(84)90003–2.

Retallack, G.J., 1998, Search for evidence of impact at the Permian-Triassic boundary in Antarctica and Australia: Geology, v. 26, p. 979–982, doi: 10.1130/0091–7613(1998)026<0979:SFEOIA>2.3.CO;2.

Riccardi, A., Kump, L.R., Arthur, M.A., and D'Hondt, S., 2007, Carbon isotopic evidence for chemocline upward excursions during the end-Permian event: Palaeogeography, Palaeoclimatology, Palaeoecology, v. 248, p. 73–81, doi: 10.1016/j.palaeo.2006.11.010.

Ries-Kautt, M., and Albrecht, P., 1989, Hopane-derived triterpenoids in soils: Chemical Geology, v. 76, p. 143–151, doi: 10.1016/0009–2541(89)90133–2.

Schönlaub, H.P., 1991, The Permian-Triassic of the Gartnerkofel-1 core (Carnic Alps, Austria): Conodont biostratigraphy, *in* Holser, W.T., and Schönlaub, G.P., eds., The Permian-Triassic boundary in the Carnic Alps of Austria (Gartnerkofel region): Abhandlungen der Geologische Bundesanstalt, v. 45, p. 79–98.

Sephton, M.A., Looy, C.V., Brinkhuis, H., Wignall, P.B., de Leeuw, J.W., and Visscher, H., 2005, Catastrophic soil erosion during the end-Permian biotic crisis: Geology, v. 33, p. 941–944, doi: 10.1130/G21784.1.

Thomas, B.M., Willink, R.J., Grice, K., Twitchett, R.J., Purcell, R.R., Archbold, N.W., George, A.D., Tye, S., Alexander, R., Foster, C.B., and Barber, C.J., 2004, Unique marine Permian-Triassic boundary section from Western Australia: Australian Journal of Earth Sciences, v. 51, p. 423–430, doi: 10.1111/j.1400–0952.2004.01066.x.

Tong, J.N., and Yang, Y., 1999, Significant progresses on the Lower Triassic conodonts, Meishan, Changxing, Zhejiang Province: Chinese Science Bulletin, v. 42, p. 2571–2573.

Uemura, H., and Ishiwatari, R., 1995, Identification of unusual 17β(H)-moret-22(29)-ene in lake sediments: Organic Geochemistry, v. 34, p. 1353–1371, doi: 10.1016/0146–6380-(95)00036-E.

Wang, C., 2007, Anomalous hopane distributions at the Permian–Triassic boundary, Meishan, China—Evidence for the end-Permian marine ecosystem collapse: Organic Geochemistry, v. 38, p. 52–66, doi: 10.1016/j.orggeochem.2006.08.014.

Watson, J.S., Sephton, M.A., Looy, C.V., and Gilmour, I., 2005, Oxygen-containing aromatic compounds in a Late Permian sediment: Organic Geochemistry, v. 36, p. 371–384, doi: 10.1016/j.orggeochem.2004.10.006.

Wignall, P.B., and Twitchett, R.J., 1996, Oceanic anoxia and the end Permian mass extinction: Science, v. 272, p. 1155–1158, doi: 10.1126/science.272.5265.1155.

Xie, S., Pancost, R.D., Yin, H., Wang, H., and Evershed, R.P., 2005, Two episodes of microbial change coupled with Permo/Triassic faunal mass extinction: Nature, v. 434, p. 494–497, doi: 10.1038/nature03396.

Manuscript received 25 April 2007
Revised manuscript received 24 July 2007
Manuscript accepted 24 July 2007

Printed in USA